Monthly Notices of the ROYAL ASTRONOMICAL SOCIETY

MNRAS **476,** L34–L38 (2018) doi:10.1093/mnrasl/sly025
Advance Access publication 2018 February 19

A model for AGN variability on multiple time-scales

Lia F. Sartori,[1⋆] Kevin Schawinski,[1⋆] Benny Trakhtenbrot,[2] Neven Caplar,[3] Ezequiel Treister,[4] Michael J. Koss,[5] C. Megan Urry[6] and Ce Zhang[7]

[1]*Institute for Particle Physics and Astrophysics, ETH Zürich, Wolfgang-Pauli-Str. 27, CH-8093 Zürich, Switzerland*
[2]*Department of Physics, ETH Zürich, Wolfgang-Pauli-Str. 27, CH-8093 Zürich, Switzerland*
[3]*Department of Astrophysical Sciences, Princeton University, Princeton, NJ 08544, USA*
[4]*Instituto de Astrofísica, Facultad de Física, Pontificia Universidad Católica de Chile, Casilla 306, Santiago 22, Chile*
[5]*Eureka Scientific Inc., 2452 Delmer St. Suite 100, Oakland, CA 94602, USA*
[6]*Department of Physics, Yale University, PO Box 201820, New Haven, CT 06520-8120, USA*
[7]*Systems Group, ETH Zurich, Universitätstrasse 6, CH-8006 Zürich, Switzerland*

Accepted 2018 February 15. Received 2018 February 12; in original form 2017 December 12

ABSTRACT

We present a framework to link and describe active galactic nuclei (AGN) variability on a wide range of time-scales, from days to billions of years. In particular, we concentrate on the AGN variability features related to changes in black hole fuelling and accretion rate. In our framework, the variability features observed in different AGN at different time-scales may be explained as realisations of the same underlying statistical properties. In this context, we propose a model to simulate the evolution of AGN light curves with time based on the probability density function (PDF) and power spectral density (PSD) of the Eddington ratio ($L/L_{\rm Edd}$) distribution. Motivated by general galaxy population properties, we propose that the PDF may be inspired by the $L/L_{\rm Edd}$ distribution function (ERDF), and that a single (or limited number of) ERDF+PSD set may explain all observed variability features. After outlining the framework and the model, we compile a set of variability measurements in terms of structure function (SF) and magnitude difference. We then combine the variability measurements on a SF plot ranging from days to Gyr. The proposed framework enables constraints on the underlying PSD and the ability to link AGN variability on different time-scales, therefore providing new insights into AGN variability and black hole growth phenomena.

Key words: galaxies: fundamental parameters – quasars: general.

1 INTRODUCTION

Variability in active galactic nuclei (AGNs) is observed or inferred at all time-scales, from hours to $>10^4$ yr. It is likely to be driven by physical processes originating at different spatial scales, from the nuclear region to the size of the galaxy.

Variability on days to decades time-scales likely arises from accretion disc instabilities, mostly observed in the optical and UV bands. The AGN behaviour on these time-scales has been studied through ensemble analysis (e.g. Sesar et al. 2006; MacLeod et al. 2010; Caplar, Lilly & Trakhtenbrot 2017). Years to decades time-scales are observed also for the so-called 'changing look AGN' or 'changing look quasars', [1] where a change in AGN type is often accompanied by a change in luminosity (CLQSO, e.g. LaMassa et al. 2015; McElroy et al. 2016; MacLeod et al. 2016; Runnoe et al. 2016; Gezari et al. 2017; Ruan et al. 2016). Possible explanations for this phenomenon include changes in accretion rate (e.g. Marin 2017). On longer time-scales, $>10^4$ yr, AGN variability is probed through extended AGN photoionised emission line regions (EELR) such as the *Voorwerpjes* (VP, e.g. Lintott et al. 2009; Gagne et al. 2011; Keel et al. 2012; Sartori et al. 2016; Keel et al. 2017; Sartori et al. 2018) or ionization and radio structures in our own Milky Way (e.g. Su, Slatyer & Finkbeiner 2010; Bland-Hawthorn et al. 2013). Such time-scales may be linked to dramatic changes in the AGN accretion state, as suggested by the viscous radial inflow time-scales in standard thin accretion discs (e.g. Shakura & Sunyaev 1973; LaMassa et al. 2015), which might happen in an analogous way to X-ray binaries (e.g. Sobolewska, Siemiginowska & Gierliński 2011). The variability features observed at different time-scales, corresponding to modulation of AGN luminosity during the active phase of supermassive black holes (SMBH) growth, may then be superimposed to longer AGN phases. Schawinski et al. (2015) suggested that SMBHs can switch on and off 100–1000 times with typical

⋆ E-mail: lia.sartori@phys.ethz.ch (LFS); kevin.schawinski@phys.ethz.ch (KS)

[1] We note that the terms 'changing look AGN' and 'changing look quasars' are used inconsistently throughout the literature, and can refer to changes both in emission line width or obscuration, as well as in luminosity.

AGN phases lasting $\sim 10^5$ yr, as supported also by some models and statistical arguments (e.g. Martini & Schneider 2003; Novak, Ostriker & Ciotti 2011; Gabor & Bournaud 2013; King & Nixon 2015).

The variability features described above span many orders of magnitude both in amplitude and time-scales. In this letter, we concentrate on the optical-UV emission from AGN accretion discs, which also illuminates gas far from the nucleus. Variability may therefore be mostly attributed to non-uniform SMBH fuelling, which can arise from physical mechanisms in place at different spatial scales. First, major galaxy mergers can trigger the fuelling of a gas reservoir through the central region (e.g. Barnes & Hernquist 1991). Internal galaxy dynamics and gas temperature can then affect how and when this gas enters the accretion disc (e.g. Hopkins & Hernquist 2006). Finally, the conversion of gravitational potential to luminosity depends on physical properties of the disc (e.g. structure and viscosity), as well as the system's reaction to perturbations (e.g. Shakura & Sunyaev 1973).

In this letter, we propose a simple phenomenological model to link and describe the variability features of actively accreting SMBHs observed at different time-scales. We assume that the observed variability is mostly driven by changes in SMBH fuelling, which near the nucleus can lead to changes in accretion rate and Eddington ratio ($L/L_{\rm Edd}$). The link is motivated by general galaxy population properties, such as the $L/L_{\rm Edd}$ distribution function (ERDF) and the power spectral density (PSD) of the $L/L_{\rm Edd}$ evolution with time. This framework allows us to test if and how variability in individual AGN can be linked to and explained by the distribution of $L/L_{\rm Edd}$ among the galaxy population.

2 FRAMEWORK AND MODEL

AGN variability is generally considered to be a stochastic process (e.g. Kelly, Sobolewska & Siemiginowska 2011). Therefore, every light curve can be interpreted as a realization of an underlying set of statistical properties. In this context, Emmanoulopoulos, McHardy & Papadakis (2013) proposed an algorithm to generate light curves based on a probability density function (PDF) describing the distribution of fluxes, and a PSD describing the distribution of time frequencies.

Motivated by these ideas, we propose that AGN variability due to changes in SMBH fuelling can be modelled starting from the PDF and the PSD of the $L/L_{\rm Edd}$ evolution with time. [2] A summary of the proposed approach is illustrated in Fig. 1. By assuming that over long enough time periods every AGN should span the same $L/L_{\rm Edd}$ range as a static snapshot of the whole AGN population, the PDF shape may be inspired by the ERDF. On the other hand, the PSD of the $L/L_{\rm Edd}$ curve is likely to have a broken power-law shape, similar to what is observed for the light curves on time-scales of hours to years (although we note that such light curves are expressed in magnitude). The bending may also be expected since variability power cannot increase indefinitely, as accretion is bounded by physical processes. Following the algorithm in Emmanoulopoulos et al. (2013), the input PSD and PDF are used to generate $L/L_{\rm Edd}$ curves, which, assuming a radiative efficiency and a description for the BH mass growth, are converted into light curves. Following a forward modelling approach, the light curves can then be used to compute observables (e.g. SF points or magnitude differences) to be compared to real observations.

[2] In the following, we will refer to the time series representing the $L/L_{\rm Edd}$ evolution with time as '$L/L_{\rm Edd}$ curve'.

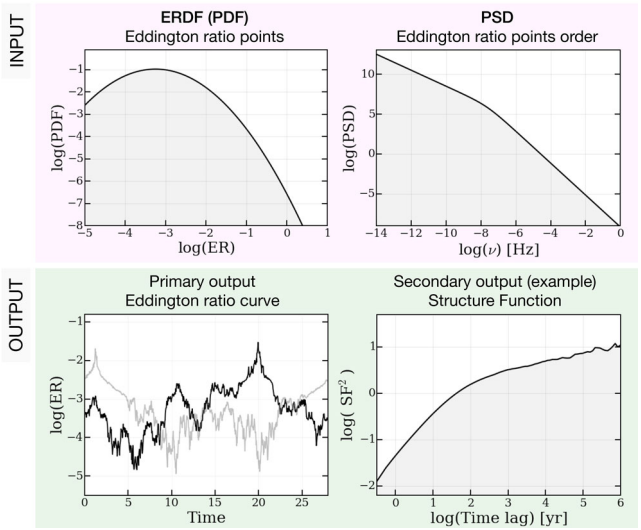

Figure 1. Schematic summary of the $L/L_{\rm Edd}$ curve simulations. The input quantities, ERDF and PSD, provide information about the $L/L_{\rm Edd}$ values allowed in the $L/L_{\rm Edd}$ curve (ERDF) and how these points are ordered (PSD). The output $L/L_{\rm Edd}$ curve (primary output; grey and black lines correspond to two different realisations) is then converted into a light curve and used to produce observables to be compared to observations (secondary output, e.g. SF). Plots are for illustrative purpose only.

In this letter, we provide a simplified proof of concept, motivated by and compared to some data available in the literature (Section 3). We will present an elaborate investigation of this model, including numerical and other tests, as well as extensive comparison with data, in a forthcoming publication. Our hypothesis is that a single ERDF+PSD set, or a limited number of them, should be able to reproduce observed light curves (in a statistical sense), that are consistent with the variability features observed both at short ($\sim$yr) and long ($>10^4$ yr) time-scales. This simple model effectively links the variability of individual AGN to the underlying, and more accessible, properties of the entire population.

3 PROOF OF CONCEPT

To show how our model can be used to link and describe AGN variability on different time-scales, we compile a set of variability measurements in terms of magnitude differences (Δm) at a given time lag, motivated by the definition of the structure function (SF). In this work, the SF^2 of the light curve $m(t_i)$ at a time lag τ is defined as

$$\mathrm{SF}^2(\tau) = \frac{1}{P}\sum_{i,j>i}\left[m(t_i) - m(t_j)\right]^2 = \langle [m(t) - m(t+\tau)]^2 \rangle, \qquad (1)$$

where P is the number of magnitude pairs $\{m(t_i),\ m(t_j)\}$ with $t_j - t_i = \tau$, and the units are [mag^2]. The SF can be computed directly from a single AGN light curve, or using an ensemble approach (e.g. MacLeod et al. 2010). From equation (1), $(\Delta m)^2$ measurements for single objects at given time-scales can be directly compared to SF^2 values. This formalism therefore allows us to compare, on a single plot, the general AGN variability behaviour at different time-scales, as well as with specific variability features (e.g. CLQSOs).

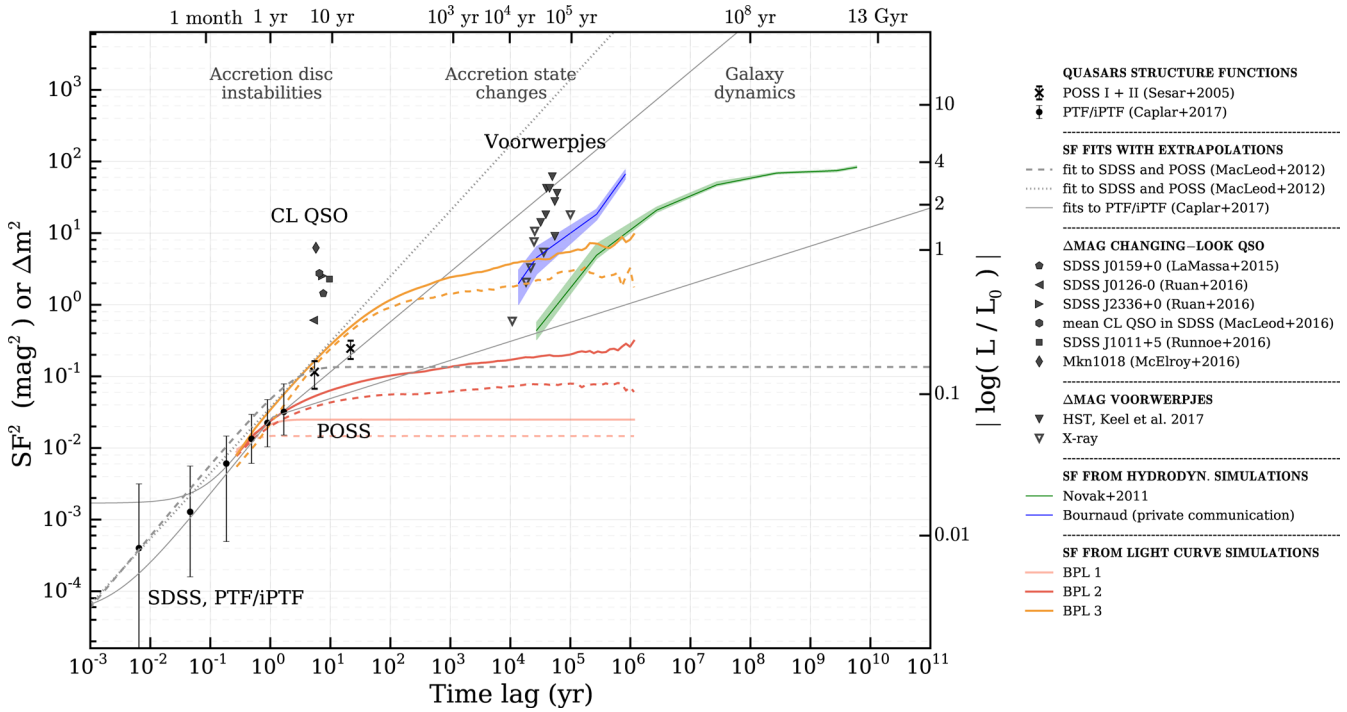

Figure 2. Rest-frame SF and Δm plot summarizing variability data from the literature and from our own estimates (black points), fits to the SF points (grey lines) as well as simulations results (coloured lines). The SF from light-curve simulations are computed both considering all the simulated points (solid line) or only the points with $L/L_{\rm Edd} > 10^{-3}$ (dashed line) to mimic observational biases. See Section 3 for details and references.

In the following, we describe how we compiled the rest-frame SF and Δm measurements shown in Fig. 2. We stress that all the measurements refer to galaxies currently hosting *actively accreting* SMBH (although EELR may, in principle, allow us to find galaxies hosting currently inactive SMBHs), and that the reported time lags correspond to the time probed by the observations, as opposed to model predictions or time-scales inferred from observed occurrence rates. Since sources generally exhibit chromatic variability properties (e.g. Vanden Berk et al. 2004), it would be preferable to compare SF and Δm in the same band. However, since the goal of this work is to compile a wide range of observations covering different time-scales, we are forced to consider measurements obtained for various spectral regimes (although we mainly concentrate on optical and UV data, which are linked to accretion disc physics and SMBH fuelling). This will not affect our main findings, as the differences among optical and UV bands are generally lower than the level of precision required for our current analysis.

3.1 Data compilation

3.1.1 Ensemble quasar variability

Ensemble SFs for time lags between days and multiple decades are often described as a damped random walk, an exponential or a broken power law (e.g. MacLeod et al. 2012; Caplar et al. 2017). In Fig. 2, we show the *r*-band SF points from the PTF/iPTF survey (Caplar et al. 2017) and the *g*-band points from POSS (Sesar et al. 2006). We also overplot example fits to the PTF/iPTF SF points (Caplar et al. 2017) and to SDSS and POSS (MacLeod et al. 2012) with extrapolation to longer time-scales. When needed we converted SF measurements and fits to agree with the formulation in equation (1).

3.1.2 Changing look QSOs

We obtained Δm values for single CLQSO from the literature, starting from the reported changes in magnitude or accretion rate (LaMassa et al. 2015; McElroy et al. 2016; Runnoe et al. 2016; Ruan et al. 2016). In addition, we computed a mean $(\Delta m)^2$ value for the SDSS CLQSOs in MacLeod et al. (2016). For the time lags, we considered the shortest reported time difference between observations that bracket the AGN class change (as defined in the correspondent literature), converted into rest-frame. We note that some of these time-scales may be upper limits.

3.1.3 Extended emission line regions - Voorwerpjes

We computed the Δm values for the VP galaxies in two different ways. For eight galaxies with available narrow-band *HST* imaging (Keel et al. 2015), we considered the difference between the observed nuclear emission and that required to account for the AGN-like emission in the most distant, AGN-photoionized region (assuming a constant spectral energy distribution shape; see Keel et al. 2017, for the ionization history reconstruction). For seven galaxies, we estimated the present day AGN luminosities from the fit to the *XMM–Newton* and *NuSTAR* X-ray spectra and a conversion factor to bolometric luminosity (Marconi et al. 2004), and compared them to the past luminosities inferred from the ionizing luminosity reported in Keel et al. (2012) (see also Sartori et al. 2018, for a similar analysis on IC 2497). The time-scales therefore correspond to the difference between the times probed by the observations. We note that since the measured distances are projected distances, the reported time lags are lower limits. Because of the complexity of photoionization physics and bolometric corrections, and the uncertainties in the travel time estimation, we caution that the obtained Δm values and time lags have to be treated as order of magnitude estimates. We also stress that, because of the sample selection,

the VP sample is biased towards AGN exhibiting large luminosity drops.

3.1.4 Hydrodynamic simulations

Most simulations that trace SMBH growth provide a history of BH accretion rates, which, in turn, can be converted into (bolometric) light curves. By assuming that the bolometric luminosity varies in the same way as the optical luminosity, the simulated light curves can be used to compute SFs to be compared with observations. In Fig. 2, we show the SFs obtained from the simulations in Novak et al. (2011) and from F. Bournaud (private communication). We note that simulations are currently the only possible way to investigate AGN variability on time-scales longer than 10^5 yr.

3.2 Example model

To illustrate a possible application of our model, we simulate $L/L_{\rm Edd}$ curves with three different input PSD and PDF, and compute their SF in magnitude space. The obtained SF can then be compared to the values in Fig. 2 to test if the input PSD and PDF can explain the observed variability.

We chose a lognormal PDF with the same parameters as the ERDF proposed in Weigel et al. (2017). For the PSD, we considered three different broken power-laws with different slopes and break frequency (BPL 1: $\alpha_{\rm low} = 0$, $\alpha_{\rm high} = -2$, $\nu_{\rm break} = 10^{-8}$ Hz $\sim$3 yr; BPL 2: $\alpha_{\rm low} = -1$, $\alpha_{\rm high} = -2$, $\nu_{\rm break} = 10^{-8}$ Hz $\sim$ 3 yr; BPL 3: $\alpha_{\rm low} = -1$, $\alpha_{\rm high} = -2$, $\nu_{\rm break} = 2 \times 10^{-10}$ Hz $\sim$160 yr). We then assumed a linear conversion between $L/L_{\rm Edd}$ and luminosity ($M_{\rm BH}$ is not expected to increase significantly during the considered time-scales) and computed the SF in magnitude space with equation (1). The resulting SF, arbitrarily renormalized to be consistent with the PTF/iPTF SF, are shown in Fig. 2. The origin of the normalization mismatch may arise, for example, from numerical effects and/or fundamental physics (see below) and will be addressed in a future work.

We caution that because of computational limits and uncertainties due, for example, to the conversion from $L/L_{\rm Edd}$ to luminosity, [3] these example simulations have illustrative purposes only. The details of the simulation approach, as well as the comparison with the data, will be addressed in detail in a forthcoming publication. The aim of the current proof of concept is not to fit the data, but rather to qualitatively illustrate what different PSDs lead to.

4 DISCUSSION

4.1 Insights and results from the structure function plot

The SF^2 and $(\Delta m)^2$ plot in Fig. 2 summarises all the observed variability measurements described in Section 3. The SF corresponding to the short time-scales probed by ensemble analysis implies an increase in variability with increasing time lags, and hints at a flattening at $\tau \sim 10^1$–10^2 yr. Extrapolating the fits to these SF measurements to longer time-scales leads to disagreement. They are therefore not sufficient to predict variability at longer, $>10^4$ yr, time-scales.

[3] The conversion from $L/L_{\rm Edd}$ to either bolometric or monochromatic luminosities is not fully understood yet, especially at low $L/L_{\rm Edd}$ regimes (ER $\ll$0.01) where we expect a change from radiative efficient to radiative inefficient accretion (e.g. Ho 2009).

The position of the VP galaxies on the plot provides further support for a flattening of the SF at time lags exceeding the regime probed by ensemble analysis. We stress that some of the VP galaxies were preselected to show large luminosity drops. Since VP are rare among general AGN population, the ensemble SF at these time-scales may be much lower. The *observed* flattening of the SF is also a natural consequence of the fact that, at long time lags, a single power law SF would predict Δm that are too large to be observed due to sensitivity limits and AGN selection criteria. Indeed, AGNs with very low $L/L_{\rm Edd}$ ($\sim 10^{-4}$ or lower) are almost undetectable with current facilities, unless they are found in nearby galaxies with high quality data. Such selection biases can be included in our modelling approach. We will therefore be able to test if a single ERDF+PSD set, or a limited number of them, can reproduce the observed flattening and variability features.

The $(\Delta m)^2$ values observed in some CLQSOs are at least one order of magnitude higher than the mean values given by the SF measured using the ensemble approach, in agreement with the results reported in many of the aforementioned CLQSO studies. Similar to what is observed for the VP, CLQSO are likely rare based on large searches (e.g. MacLeod et al. 2016; Ruan et al. 2016) and possibly related to other processes with higher variability. Modelling the AGN light curves and the $(\Delta m)^2$ distributions may help understand if these objects are the extreme tail of the AGN phenomena, or if they represent a separate process (see Graham et al. 2017; Rumbaugh et al. 2017, for a discussion about extreme variability in QSO).

The variability properties predicted by hydrodynamic simulations are strongly dependent on their spatial resolution and on the applied accretion and feedback recipes. This is consistent with the fact that the BH fueling, and thus variability in emission, is ultimately dominated by circumnuclear processes, on scales that are seldom addressed by simulations. Current hydrodynamic simulations are therefore not suited to investigate AGN variability. Fig. 2 illustrates the challenges that simulations are facing (e.g. Negri & Volonteri 2017), and provides an additional way to test how closely future simulations will reflect observations.

4.2 Insights from modelling

In Section 3.2, we outlined an example application of our method. We considered three different ERDF+PSD sets. The first results suggest that a broken power-law shaped PSD may be able to explain the gross variability features observed. However, further investigation – for example, of the input definition and conversion from $L/L_{\rm Edd}$ curves to observables – is needed to get more constraining results. This will be addressed in detail in a forthcoming paper.

We hypothesize that a single ERDF+PSD set, or a limited number of them, should be able to produce $L/L_{\rm Edd}$ curves, and therefore accretion rate and light curves, which are consistent with the observed variability features both at short ($\sim$yr) and long ($>10^4$ yr) time-scales. This assumption may be justified by the fact that the ERDF appears to be universal (Weigel et al. 2017), and by the BH accretion physics (e.g. Shakura & Sunyaev 1973). Since there is no obvious reason that accretion disc physics should evolve with time (the same physics is expected in local galaxies and in z $\sim$ 7 quasars), the short time-scale variations connected to the accretion disc ought to be redshift independent. On the other hand, the long-time-scale variability linked to cosmology may evolve with redshift (e.g. redshift-dependent gas accretion or merger rate, Lotz et al. 2011). In any case, since the observations in Fig. 2 are mostly for luminous quasars in low to intermediate redshift galaxies, we cannot probe the evolution

with redshift with the current data. We also note that, as suggested by some ensemble studies (e.g. Caplar et al. 2017; Rumbaugh et al. 2017), short time-scale variability could depend on $L/L_{\rm Edd}$, luminosity and black hole mass $M_{\rm BH}$. However, the data analysed here do not seem to require a model dependent on these quantities. We will investigate this aspect further in future studies.

If our hypothesis is correct, the underlying PSD would be the temporal analogue in AGN physics to the matter power spectrum in cosmology: similarly to how a single matter power spectrum is responsible for multiple matter assemblages (e.g. Frenk & White 2012), from large cosmic structures down to dwarf galaxies, the AGN power spectrum may be responsible for AGN variability over many orders of magnitude in time. If this is true, our model will allow us to link and describe AGN variability at different time-scales. Our framework will allow us to test this hypothesis and to constrain the shape of the underlying PSD, providing novel insights into the AGN variability phenomenon.

ACKNOWLEDGEMENTS

We acknowledge support from SNSF Grants PP00P2_138979 and PP00P2_166159 (LS, KS); NASA through ADAP award NNH16CT03C (MJK); CONICYT grant Basal-CATA PFB-06/2007; and FONDECYT Regular 1160999 (ET).

REFERENCES

Barnes J. E., Hernquist L. E., 1991, ApJ, 370, L65
Bland-Hawthorn J., Maloney P. R., Sutherland R. S., Madsen G. J., 2013, ApJ, 778, 58
Caplar N., Lilly S. J., Trakhtenbrot B., 2017, ApJ, 834, 111
Emmanoulopoulos D., McHardy I. M., Papadakis I. E., 2013, MNRAS, 433, 907
Frenk C. S., White S. D. M., 2012, Annalen der Physik, 524, 507
Gabor J. M., Bournaud F., 2013, MNRAS, 434, 606
Gagne J., Crenshaw D. M., Keel W. C., Fischer T. C., 2011, Am. Astron. Soc. Meeting Abst. #217, 142.12
Gezari S. et al., 2017, ApJ, 835, 144
Graham M. J., Djorgovski S. G., Drake A. J., Stern D., Mahabal A. A., Glikman E., Larson S., Christensen E., 2017, MNRAS, 470, 4112
Ho L. C., 2009, ApJ, 699, 626
Hopkins P. F., Hernquist L., 2006, ApJS, 166, 1
Keel W. C. et al., 2012, MNRAS, 420, 878
Keel W. C. et al., 2015, AJ, 149, 155
Keel W. C. et al., 2017, ApJ, 835, 256
Kelly B. C., Sobolewska M., Siemiginowska A., 2011, ApJ, 730, 52
King A., Nixon C., 2015, MNRAS, 453, L46
LaMassa S. M. et al., 2015, ApJ, 800, 144
Lintott C. J. et al., 2009, MNRAS, 399, 129
Lotz J. M., Jonsson P., Cox T. J., Croton D., Primack J. R., Somerville R. S., Stewart K., 2011, ApJ, 742, 103
MacLeod C. L. et al., 2010, ApJ, 721, 1014
MacLeod C. L. et al., 2012, ApJ, 753, 106
MacLeod C. L. et al., 2016, MNRAS, 457, 389
Marconi A., Risaliti G., Gilli R., Hunt L. K., Maiolino R., Salvati M., 2004, MNRAS, 351, 169
Marin F., 2017, A&A, 607, A40
Martini P., Schneider D. P., 2003, ApJ, 597, L109
McElroy R. E. et al., 2016, A&A, 593, L8
Negri A., Volonteri M., 2017, MNRAS, 467, 3475
Novak G. S., Ostriker J. P., Ciotti L., 2011, ApJ, 737, 26
Ruan J. et al., 2016, ApJ, 826, 188R
Rumbaugh N. et al., 2017, ApJ, 854, 160
Runnoe J. C. et al., 2016, MNRAS, 455, 1691
Sartori L. F. et al., 2016, MNRAS, 457, 3629
Sartori L. F. et al., 2018, MNRAS, 474, 2444
Schawinski K., Koss M., Berney S., Sartori L. F., 2015, MNRAS, 451, 2517
Sesar B. et al., 2006, AJ, 131, 2801
Shakura N. I., Sunyaev R. A., 1973, A&A, 24, 337
Sobolewska M. A., Siemiginowska A., Gierliński M., 2011, MNRAS, 413, 2259
Su M., Slatyer T. R., Finkbeiner D. P., 2010, ApJ, 724, 1044
Vanden Berk D. E. et al., 2004, ApJ, 601, 692
Weigel A. K., Schawinski K., Caplar N., Wong O. I., Treister E., Trakhtenbrot B., 2017, ApJ, 845, 134

This paper has been typeset from a TEX/LATEX file prepared by the author.